Purdue University
Purdue e-Pubs

International High Performance Buildings
Conference

School of Mechanical Engineering

July 2018

Thermoelectric Heat Pump Clothes Dryer using Secondary Loop Heat Exchangers: Experimental Evaluation and System Modeling

Viral Patel
Oak Ridge National Laboratory, United States of America, patelvk@ornl.gov

Kyle R Gluesenkamp
Oak Ridge National Laboratory, United States of America, gluesenkampk@ornl.gov

Follow this and additional works at: https://docs.lib.purdue.edu/ihpbc

Thermoelectric Heat Pump Clothes Dryer using Secondary Loop Heat Exchangers: Experimental Evaluation

Viral K. PATEL*, Kyle R. GLUESENKAMP

Oak Ridge National Laboratory[1]
Oak Ridge, TN, USA
patelvk@ornl.gov, gluesenkampk@ornl.gov

* Corresponding Author

ABSTRACT

Past work has shown that thermoelectric clothes dryers are capable of much higher efficiency than electric resistance clothes dryers. In an effort to improve performance and reduce material utilization, this work explores a new secondary loop system configuration. In this configuration, heat is transferred between air and the thermoelectric heat pumps via two water loops and two water-to-air fin-tube type heat exchangers. In this work, performance is investigated and analyzed using experimental data.
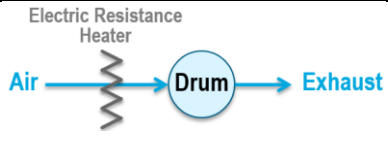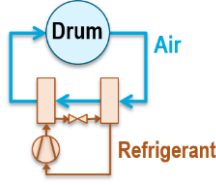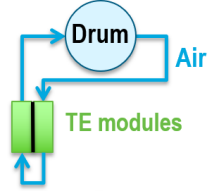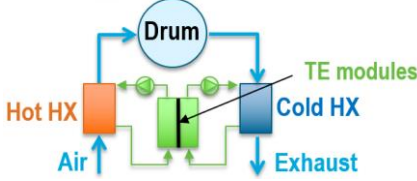
1   INTRODUCTION

Electric clothes dryers in the US have an annual primary energy consumption of approximately 620 TBtu (182 TWh) [1]. The vast majority of clothes dryer technology is based on inefficient electric resistance (ER) heating. Although dryers with superior energy efficiency (such as vapor compression heat pump (VCHP) dryers) exist on the market, their availability in the US is limited. Recent research being conducted to improve the efficiency and performance of clothes dryers includes further development of VCHP dryers [2, 3], improvements in the design of the electric heating elements in conventional ER dryers [4], using water-cooled heat exchangers to enhance condensation in condensing ER dryers [5] and using heat pipe-based heat exchangers to recover exhaust heat in ER dryers [6].

As an alternative to VCHP dryers, thermoelectric (TE) heat pump clothes dryers have also been studied recently with promising results [7-10]. As opposed to vapor-compression cycles that use refrigerant, TE dryers rely on solid-state thermoelectric technology to achieve heat pumping. Due to the Peltier effect, applying a voltage across a TE module results in a temperature difference between the two side of the module, allowing it to effectively pump heat [11]. Commercially available TE modules have a wide range of form factors, capacities, operating temperatures and efficiency and can be combined in a multitude of ways to provide the heating and cooling capacity necessary for clothes drying applications. The typical configurations and performance of prior and current TE dryers are compared to baseline ER dryers and state-of-the-art VCHP dryers in Table 1. The energy factor is a measure of the clothes dryer efficiency; the higher the value, the more efficient the clothes dryer is.

Table 1. Air flow configurations, typical energy factors and dry times for various electric clothes dryer technologies

Clothes dryer type	Typical configuration	Typical energy factor	Typical dry time
Baseline: Electric resistance (ER)	Electric Resistance Heater — Air → Drum → Exhaust	3.73 lb_{BDW}/kWh	15 – 30 min
State-of-the-art: Vapor compression heat pump (VCHP)	Drum — Air — Refrigerant	4.3 – 6.4 lb_{BDW}/kWh	57 – 75 min
Prior work: Thermoelectric heat pump – air based [7-10]	Drum — Air — TE modules	6.03 lb_{BDW}/kWh obtained experimentally	120 min
Current work: Thermoelectric heat pump – pumped loop*	Drum — Hot HX — TE modules — Cold HX — Air — Exhaust	5.4 lb_{BDW}/kWh obtained experimentally	80 min

*Patent pending [12]

As shown in Table 1, the initial air-based TE dryer development [7-10] resulted in up to 38% improvement in energy factor compared to that of baseline ER dryers, similar to that of VCHP dryers. However, the dry time was substantially longer due to limitations in heat and mass transfer associated with the air-based design. In addition to this, the air-based design required the use of heat sinks with high air-side pressure drop and substantial mass, increasing the overall system costs.

To improve the performance and material utilization of TE dryers, the current work explores a new configuration that utilizes pumped secondary loops with conventional fin-and-tube heat exchangers. Although the system complexity is increased compared to the air-based design, the use of optimized heat exchangers and hydronic pumped loops which have high heat and mass transfer effectiveness is expected to significantly reduce the dry time, bringing it in line with the state-of-the-art dryers available today.

2 EXPERIMENTAL SETUP

2.1 Process and instrumentation diagram

The experimental design specifications for the pumped loop TEHP dryer prototype were based on detailed modeling and experimental results from the previous generation air-based TE clothes dryer [7-10]. The current experimental setup consisted of a modified ER dryer with temperature, pressure, relative humidity (RH) and flow sensors installed, as illustrated in the process and instrumentation diagram in Figure 1. The block arrows show the air flow path and direction, while the dashed line arrows show the water flow path and direction in the hot and cold secondary loops.
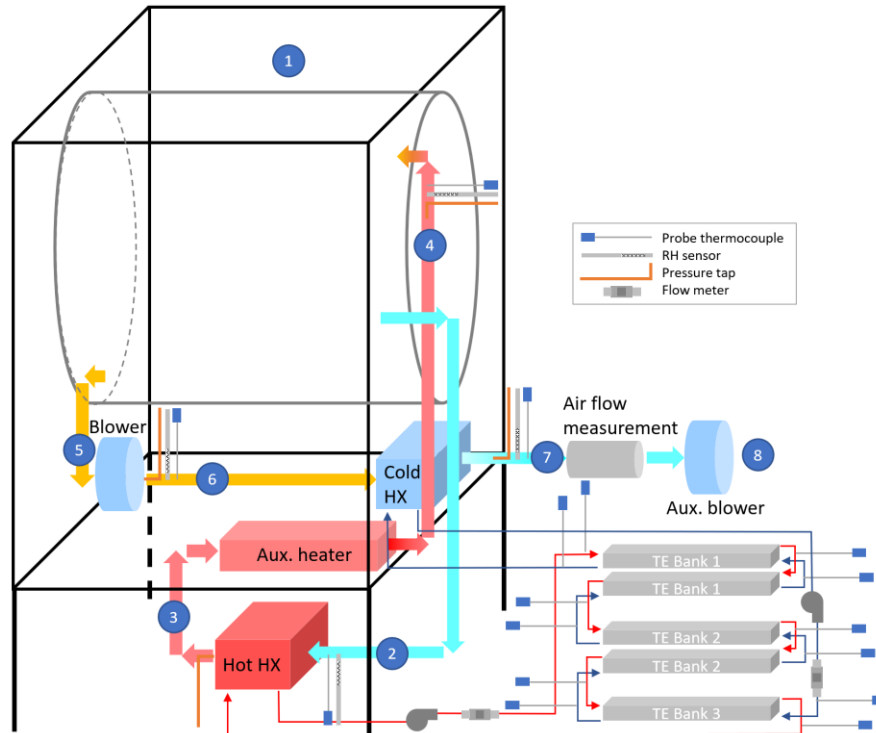
Figure 1. Process and instrumentation diagram for TE clothes dryer prototype

A once-through (i.e. vented) air flow path was used, as opposed to the closed-loop (i.e. ventless) air flow. Air was first drawn from the dryer cabinet at state point ① and entered the hot fin-and-tube heat exchanger (hot HX) at state point ②. Hot water circulating through the hot HX was used to raise the temperature of the air (details of the TE heat pump assembly and secondary loops are provided in Section 2.2). The air exited the hot HX at state point ③ and entered the auxiliary ER heater which had a capacity of 1 kW and was not activated for most trials. The air entered the dryer drum at state point ④ and gained moisture from the tumbling wet fabric. It then exited the drum (through the lint filter) and entered the blower at state point ⑤. It exited the blower and entered the cold fin-and-tube heat exchanger (cold HX) at state point ⑥. Cold water circulating through the cold HX resulted cooled the exhaust air. The air exited the cold HX and entered a traversing pitot station (for air flow rate measurement) at state point ⑦. It then flowed through the auxiliary blower (used to boost overall air flow rate) before being vented to the ambient at state point ⑧.

2.2   TE heat pump and secondary loop design

The TE heat pump assembly was made up of five TE arrays, with each array having five TE modules (resulting in a total of 25 TE modules) with each array sandwiched between two aluminum mini-channel heat exchangers. As water flowed through the top mini-channel HXs, it was heated up by the hot sides of the TE modules. At the same time, water flowing through the bottom mini-channel HXs was cooled down by the cold sides of the TE modules. As illustrated in Figure 1, the top and bottom mini-channel HXs were all connected in series with each other, with the hot-side secondary loop connected to the hot fin-and-tube HX and cold-side secondary loop connected to the cold fin-and-tube HX. A CAD model of a pair of TE arrays is shown in Figure 2, with arrows indicating the flow direction of the hot and cold water into and out of the manifolds. Aluminum spacer blocks were used to separate the top and bottom mini-channel HXs.
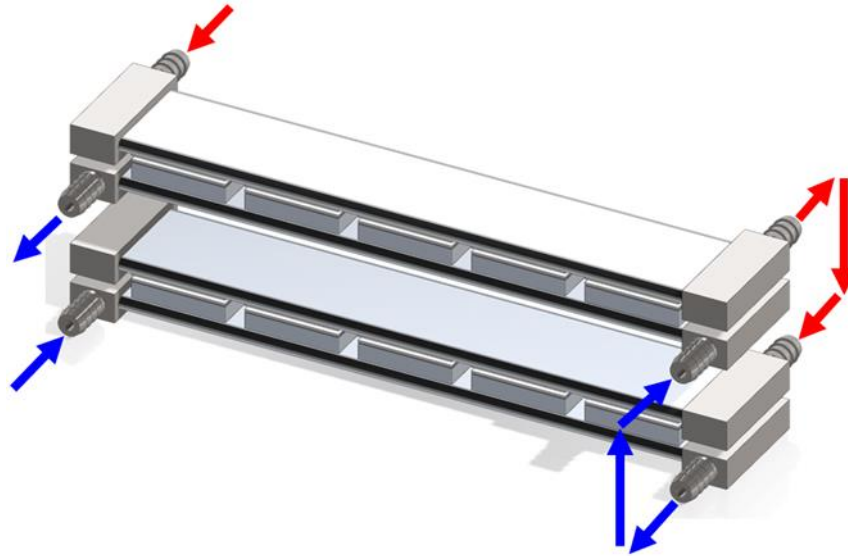
Figure 2. CAD model of a pair of TE arrays with arrows indicating the flow direction of hot and cold water

A cross-sectional view of a TE module sandwiched between two mini-channel HXs is shown below in Figure 3, along with the important thermal resistances and heat transfer path.
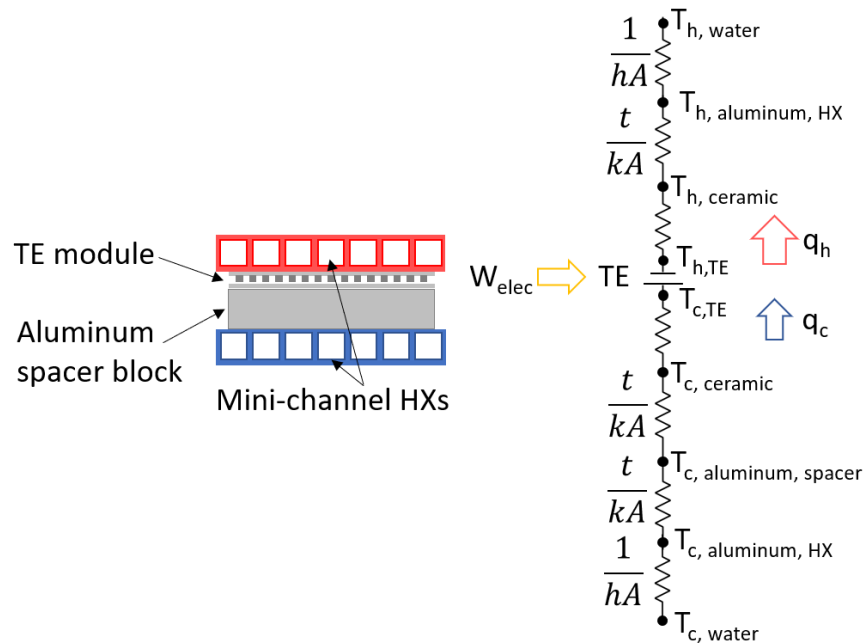

Figure 3. Cross-sectional view and thermal resistance diagram of TE module and mini-channel HXs

In Figure 3, W_{elec} is the electrical work input to the TE module, T_h is the hot-side temperature, T_c is the cold-side temperature, q_h is the heating capacity, q_c is the cooling capacity, t is material thickness, A is heat transfer surface area, k is thermal conductivity and h is the water convective heat transfer coefficient.

2.3   Measurement and control

Measurements of applied voltage and current flowing through the TE modules were used to determine the TE power input.

The water flow rate in the secondary loops was controlled by two variable voltage DC pumps. The volumetric flow rate was measured using turbine flow meters and could be precisely adjusted to achieve the desired flow rate. The

system air flow was boosted by a small auxiliary blower. Air flow rate remained relatively constant for the duration of the tests. It was measured using a pitot traverse station paired with a differential pressure transducer.

For each trial, the fabric test load was weighed on a small scale three times: after bone-drying in a separate dryer, after wetting to 57.5% moisture content, and finally at the end of the trial. In addition to this, the entire TE clothes dryer prototype was placed onto a floor scale to measure the whole dryer mass as it changed during the test. This allowed the instantaneous moisture content of the fabric to be ascertained and provided a precise stopping point for the trials. Details of other measurement instruments used in the TE clothes dryer prototype are given in Table 2, along with their maximum uncertainties.

Table 2. Instrument uncertainties for TE clothes dryer prototype

Quantity	Instrument	Maximum uncertainty
Temperature	Omega TMQSS-06U-6 Type T thermocouple	± 0.5°C
Static pressure	Setra Model 264 Very low differential pressure transducer	± 7.5 Pa
Air flow rate	Air Monitor Corp. Veltron DPT2500 Transmitter with 4" LO-flo Pitot Traverse Station	± 3 % rdg.
Water flow rate	Omega FTB-430 Turbine flow meter	± 2 % rdg.
Dewpoint temperature	Vaisala HMT 330 Transmitter with HMT 337 warmed probe	± 0.67°C
Applied voltage to TE banks	Sorensen XG150-5.6 DC Programmable Power Supply	± 2.18 V
Current through TE banks	Sorensen XG150-5.6 DC Programmable Power Supply	± 0.056 A
Blower/drum rotator motor power	Ohio Semitronics PC5-010DY25 AC Watt Transducer	± 5 W
Mass of test load	Sartorius Midrics 1	± 2 g
Mass of whole dryer	Mettler Toledo 2158 MT 500LB 30X30 5KD	± 45 g

2.4   Completed TE clothes dryer prototype

The CAD model and completed TE clothes dryer prototype are shown in Figure 4. The modified ER dryer was installed on top of a support stand with a shelf to hold the TE heat pump assembly, hot HX, tubing, water pumps and flow meters. The cold HX and auxiliary heater were located inside the dryer cabinet.
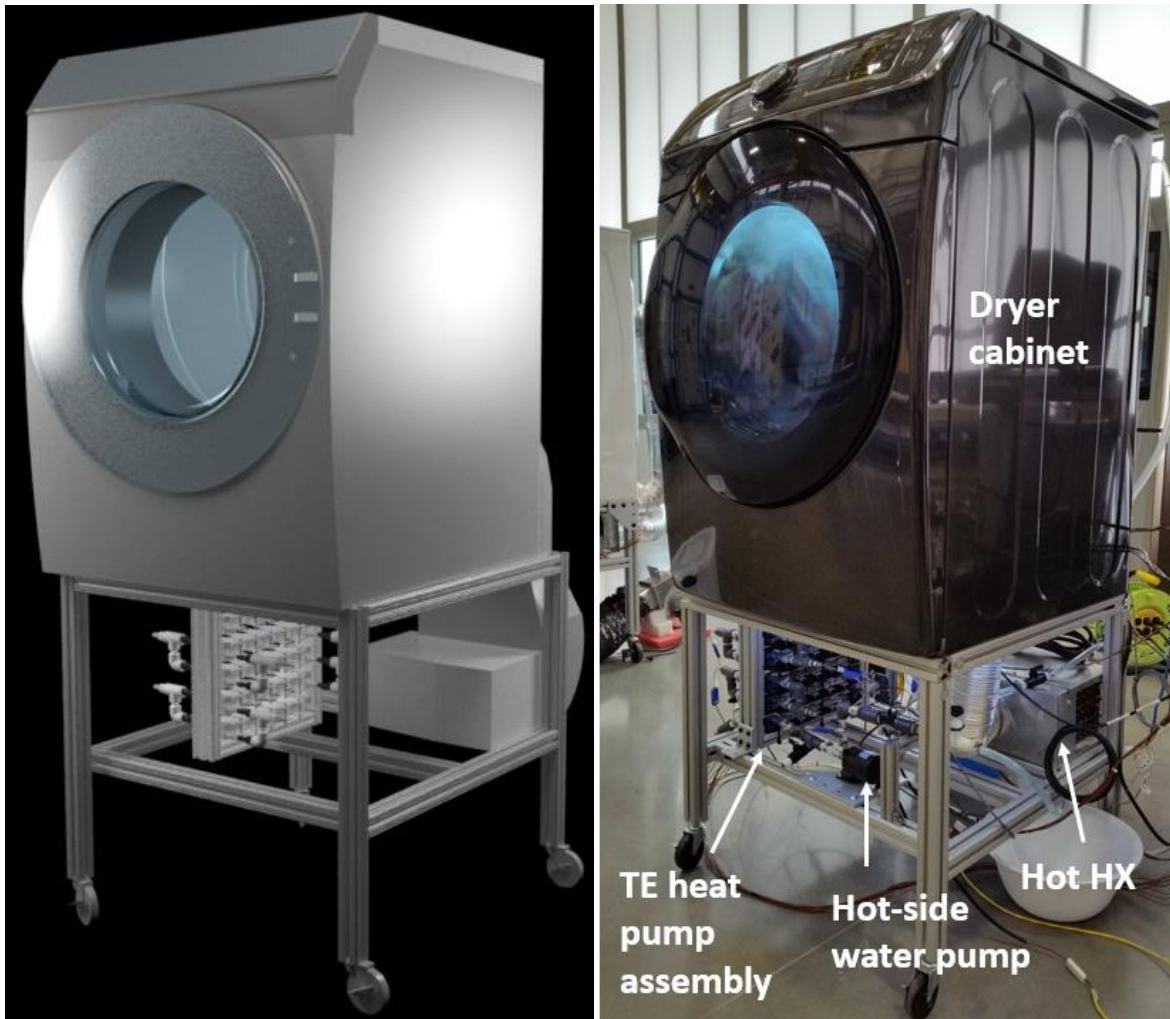
Figure 4: CAD model (left) and completed pumped loop TE clothes dryer prototype (right, patent pending [12])

3   RESULTS AND DISCUSSION

Experimental trials were conducted according to the standard test procedure for residential clothes dryers outlined in 10 CFR 430 [13]. The load bone dry weight (BDW) was first verified using a scale. Trials were conducted for three different load sizes: a compact load (BDW = 3.00 lb.), a standard load (BDW = 8.45 lb.) and a large load (BDW = 16.9 lb.). A conventional washing machine was used to uniformly wet the fabric, using the rinse and spin cycles. The starting moisture content (SMC), calculated using bone dry weight and wet weight, was adjusted until it was at 57.5 ± 0.33%. The wet fabric was then loaded in the TE dryer prototype to begin the experiment. The drum rotator motor and blowers were started, and the TE bank power supplies were activated. All measurements were recorded at a rate of 1 sample/sec. The experiment was continued until the final moisture content (FMC) was less than 4%. As a measure of the clothes drying efficiency, the combined energy factor (CEF) was computed for all trials. To compute CEF, the bone-dry weight (in lb.) of the cloth was divided by the energy used during the drying process (in kWh). This energy included the AC electrical energy consumption of the TE power supplies (a conversion efficiency of 90% was assumed to account for AC to DC conversion losses), main blower/drum rotator motor and auxiliary blower and DC electrical energy consumption of the water pumps. The CEF was compared for all trials, with a high relative value of CEF signifying high energy efficiency for a given trial.

A total of nine experimental trials were conducted, with variation in load size, current applied to TE banks and auxiliary heater use (on or off). Example measurements from trial 4 are given in Figure 5 to illustrate some of the experimental data that were acquired during testing.
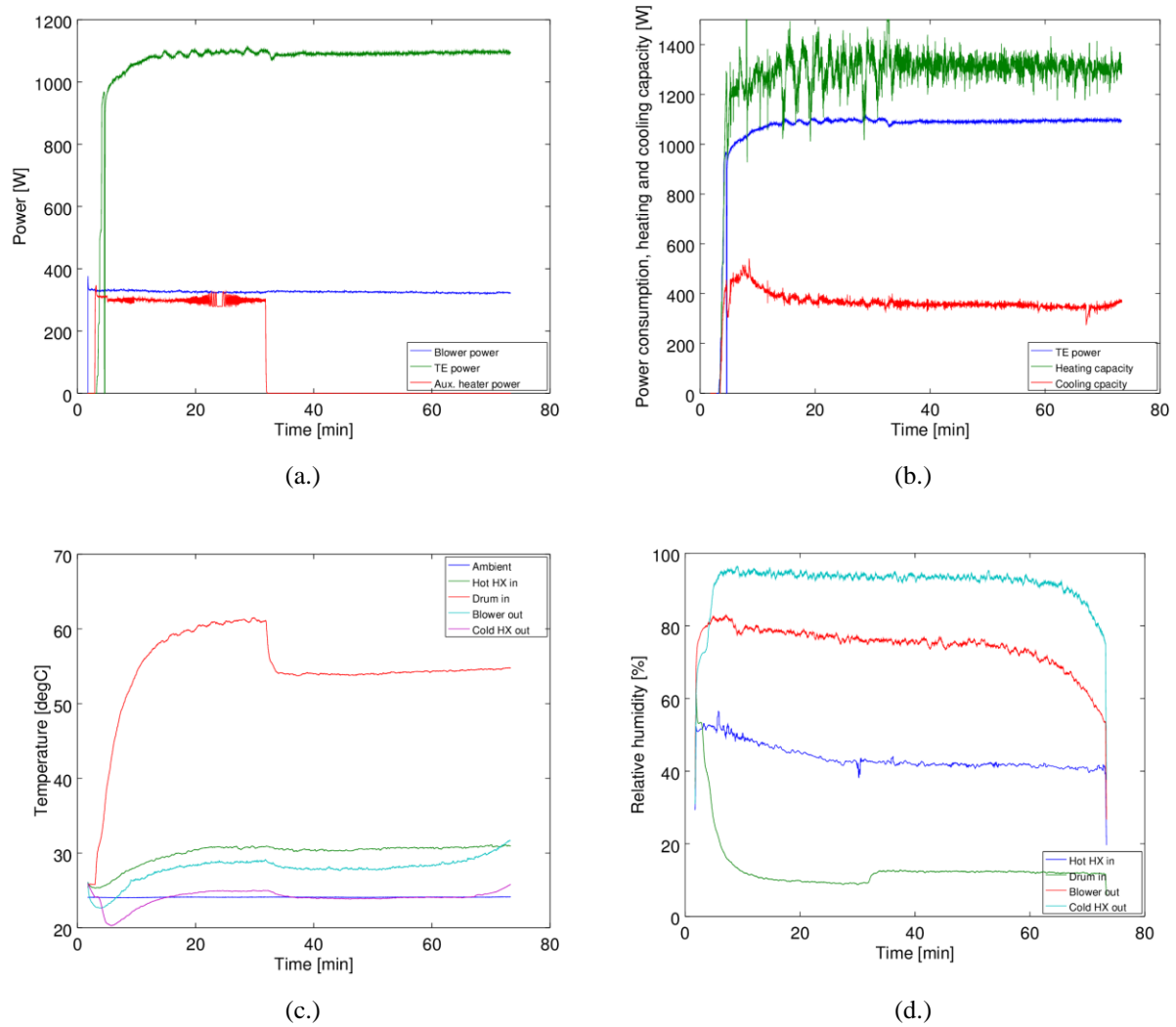
(a.)

(b.)

(c.)

(d.)

Figure 5. Plots of (a.) electric power consumption, (b.) Water-side heating and cooling capacity, (c.) air temperatures at various state points, (d.) RH at various state points vs. time for trial 4

The average TE power input was 1051 W for trial 4, as shown in Figure 5a. For this trial, the auxiliary heater was activated for the first 30 min (with 300 W applied) and then deactivated for the remainder of the test. The heating and cooling capacities in Figure 5b were determined using the hot and cold water flow rates and inlet-outlet temperature differences in the secondary loops of the TE heat pump. A summary of the nine trials conducted so far is given in Table 3 and a plot of CEF vs. dry time is given in Figure 6. As noted above, the CEF was calculated using the fabric bone dry weight and energy consumed to dry the fabric from SMC ≈ 57.5% to FMC ≤ 4%, denoted "Ece" in Table 3.

Table 3. Summary of nine trials conducted for TE clothes dryer prototype

| Trial #	Load size BDW [lb]	SMC [%]	FMC [%]	Average AC TE power [W]	Average AC blower + drum motor power [W]	Average AC aux. heater power [W]	Average approx. DC pump power [W]	Dry time [min]	Ece for CEF [kWh]	CEF [lb_BDW/kWh]
1	8.45	57.38	2.66	545.63	340.55	0	10	110	1.67	5.05
2	8.37	57.45	2.63	1066.52	326.36	0	23	80	1.92	4.36
3	8.43	57.22	3.56	1100.56	328.14	0	23	75	1.89	4.47
4	8.43	57.32	3.97	1050.97	325.41	120.69	7.3	71.6	1.88	4.49
5	2.99	57.58	3.53	1029.23	312.13	0	7.3	33	0.77	3.91
6	8.43	57.32	4.07	1082.24	326.47	0	7.3	71.5	1.77	4.77
7	8.41	57.37	3.20	1066.93	335.74	0	7.3	71.6	1.73	4.86
8	16.94	57.35	2.89	1107.63	357.72	0	7.3	139.6	3.51	4.83
9	8.41	57.32	3.15	798.22	337.35	0	7.3	79.5	1.56	5.40
10	8.41	57.32	3.36	1366.61	335.24	0	7.3	68.55	2.02	4.17
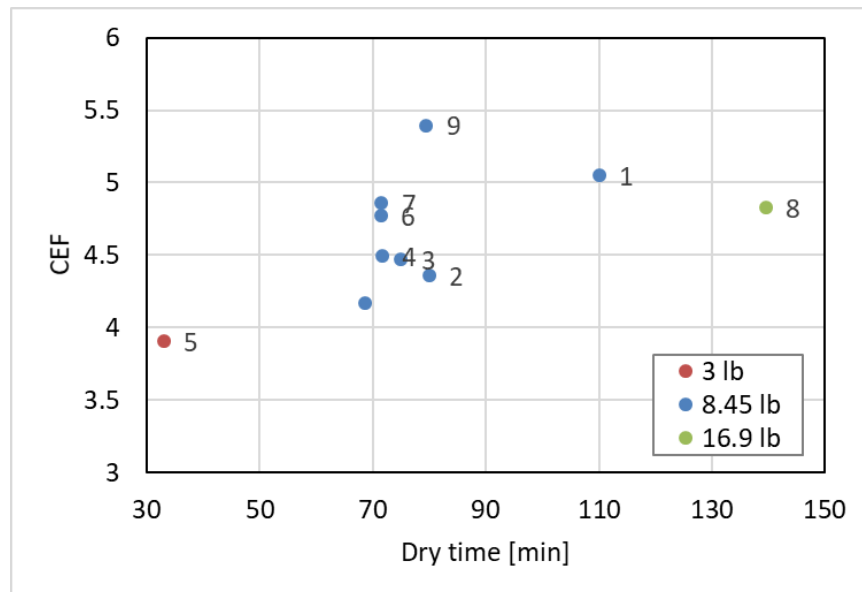
Figure 6. Combined energy factor (CEF) vs. dry time for nine trials and varying test load size

As the above trials were conducted, component and duct insulation was improved, air leakages into the system were sealed and water in the secondary loops was deaerated. Although minor, these changes had a marked effect on the system performance, as evidenced by the steady increase in CEF for sequential trials with standard 8.45 lb loads.. The above results in Table 3 and Figure 6 show that the new pumped loop TE clothes dryer prototype is capable of drying standard loads of fabric with significantly higher CEF compared to baseline EF dryers (as much as 31% higher) with reasonable dry times. For the compact load size of 3.00 lb., the drying time can be as low as 33 min, at the expense of CEF. For the large load, CEF is similar to that of standard load trials, but dry time is increased by 60 – 70 min.

4   CONCLUSIONS

A new configuration of TE clothes dryers was studied in this work that utilized pumped secondary loops and conventional fin-and-tube heat exchangers. Building upon previous success with air-based TE dryer design, the current TE dryer prototype has demonstrated a CEF of 5.40 lb_BDW/kWh with a dry time of 80 min for standard load size of 8.45 lb. This is a 31% improvement in CEF over baseline ER dryers. The results achieved are similar to the state-of-the-art VCHP dryers, with further improvement in efficiency and dry time expected. The next steps in the research are to continue testing with variation in control strategy and air flow rate and to identify design and component changes to improve performance.

ACKNOWLEDGEMENTS

REFERENCES

[1] EIA, 2018, "Baseline Energy Calculator," https://trynthink.github.io/scout/calculator.html, U.S. Energy Information Administration.

[2] Bellomare, F., and Minetto, S., 2015, "Experimental Analysis of Hydrocarbons as Drop-in Replacement in Household Heat Pump Tumble Dryers," Energy Procedia, 81, pp. 1212-1221.

[3] TeGrotenhuis, W., Butterfield, A., Caldwell, D., Crook, A., and Winkelman, A., 2017, "Modeling and design of a high efficiency hybrid heat pump clothes dryer," Applied Thermal Engineering, 124, pp. 170-177.

[4] Zhao, J., Jian, Q., Zhang, N., Luo, L., Huang, B., and Cao, S., 2018, "The improvement on drying performance and energy efficiency of a tumbler clothes dryer with a novel electric heating element," Applied Thermal Engineering, 128, pp. 531-538.

[5] Qifei, J., and Jing, Z., 2017, "Drying performance analysis of a condensing tumbler clothes dryer with a unique water cooled heat exchanger," Applied Thermal Engineering, 113, pp. 601-608.

[6] Jian, Q., and Luo, L., 2018, "The improvement on efficiency and drying performance of a domestic venting tumble clothes dryer by using a heat pipe heat recovery heat exchanger," Applied Thermal Engineering, 136, pp. 560-567.

[7] Patel, V. K., Goodman, D., Gluesenkamp, K., and Gehl, A., 2016, "Experimental Evaluation and Thermodynamic System Modeling of Thermoelectric Heat Pump Clothes Dryer," Proc. 16th International Refrigeration and Air Conditioning Conference at Purdue, West Lafayette, IN.

[8] Goodman, D., Patel, V. K., and Gluesenkamp, K., 2017, "Thermoelectric heat pump clothes dryer design optimization," Proc. Proc. 12th IEA Heat Pump Conference, Rotterdam, The Netherlands.

[9] Patel, V. K., and Gluesenkamp, K. R., 2017, "Development of Packaging and Modular Control of Thermoelectric Clothes Dryer, With Performance Evaluation," Proc. ASME 2017 International Technical Conference and Exhibition on Packaging and Integration of Electronic and Photonic Microsystems collocated with the ASME 2017 Conference on Information Storage and Processing Systems, American Society of Mechanical Engineers, pp. V001T004A009-V001T004A009.

[10] Patel, V. K., Gluesenkamp, K. R., Goodman, D., and Gehl, A., 2018, "Experimental evaluation and thermodynamic system modeling of thermoelectric heat pump clothes dryer," Applied Energy, 217, pp. 221-232.

[11] Rowe, D. M., 2005, Thermoelectrics Handbook: Macro to Nano, CRC press - Taylor & Francis Group, Boca Raton, FL.

[12] Wu, G., Gluesenkamp, K. R., Patel, V. K., and Vaidhyanathan, R., 2018, Apparatus and Method for a Thermoelectric Heat Pump Appliance with Secondary Fluid Loops, USPTO, Application number 62/654,239, April 6, 2018

[13] 10 CFR 430, 2017, "Energy Conservation Program for Consumer Products," Subpart C, Energy and Water Conservation Standards"